논문 2000-9-4-08

백색광 간섭기에서 간섭 무늬의 상호 상관관계 함수를 이용한 절대 위상 측정 알고리즘

김 정 곤

Absolute phase identification algorithm in a white light interferometer using a cross-correlation of fringe scans

Jeong Gon Kim

요 약

본 논문에서는 백색광 간섭현상 (white light interferometry)을 위한 신호처리 알고리즘을 제안한다. 제안하는 알고리즘으로 간섭기의 광경로 절대길이 (absolute optical path length)를 정확하게 측정할 수 있다. 그리고 제안하는 알고리즘은 간섭 무늬 (fringe scan)의 상호 상관관계 함수 (cross-correlation function)와 가설 검증을 사용한다. 가설 검증은 간섭 무늬의 상호 상관관계 함수가 대칭이 되는 봉우리를 영차 간섭 봉우리 (zero order fringe peak) 후보자로 선정함으로써 영차 간섭 봉우리를 오판할 확률을 줄인다. 산탄잡음 (shot noise)이 제안된 알고리즘의 성능에 미치는 영향을 컴퓨터 모의 실험을 통하여 조사하였다. 모의 실험 결과와 보외법 (extrapolation)을 사용하여 신호대산탄잡음비 (signal-to-shot noise ratio)가 31 dB 보다 클 때의 알고리즘의 성능을 예측하였다. 간섭 봉우리 의 세 가지 매개변수 변화 (신호대산탄잡음비, 간섭 스캔 샘플링율, 광원의 가간섭성 길이)에 따른 영차 간섭 봉우리 추정 오차를 계산하였다. 모의 실험 결과를 통하여 제안한 알고리즘이 영차 간섭 무늬 봉우리를 정확하게 판별할 수 있음을 보여 주었다. 제안하는 신호 처리 알고리즘은 소프트웨어적인 기법으로서 경제적이고 속도가 빠르며 간단한 알고리즘이다.

Abstract

A new signal processing algorithm for white light interferometry has been proposed and investigated theoretically. The goal of the algorithm is to determine the absolute optical path length of an interferometer with very high precision (<< one optical wavelength). The algorithm features cross-correlation of interferometer fringe scans and hypothesis testing. The hypothesis test looks for a zero order fringe peak candidate about which the cross-correlation is symmetric minimizing the uncertainty of misidentification. The shot noise limited performance of the proposed signal processing algorithm has been analyzed using computer simulations. Simulation results were extrapolated to predict the misidentification rate at Signal-to-Shot noise ratio (SNR) higher than 31 dB. Root-mean-square phase error between the computer-generated zero order fringe peak and the estimated zero order fringe peak has been calculated for the changes of three different parameters (SNR, fringe scan sampling rate, coherence length of light source). Results of computer simulations showed the ability of the proposed signal processing algorithm to identify the zero order fringe peak correctly. The proposed signal processing algorithm uses a software approach, which is potentially inexpensive, simple and fast.

한세대학교 정보통신공학과 (Dept. of Information and Communication Eng., Hansei University)

<접수일자 : 2000년 6월 12일>

I. Introduction

For the last decade fiber optic interferometric sensors have found a wide range of applications in industrial, military and commercial fields[1],[2]. Although fiber optic interferometric sensors offer the possibility to perform measurements with very high sensitivity and resolution[3], the problems encountered are complex signal processing techniques, quadrature point stabilization, uncertainty as to whether an increase or decrease in the value of measurand and zero sensitivity problem of the maximum or minimum operating point on the transfer function curve. Furthermore, the interference fringe visibility of an interferometer with a high-coherence light source is constant regardless of the Optical Path length Difference (OPD) between the two arms of the interferometer. In this case, there will be no chance to know the OPD between two arms of the interferometer. The absolute value of the measurands cannot, therefore, be ascertained when the sensor is initialized without some form of calibration procedure[4]. In order to fully utilize the capability of fiber optic sensors, a different sensing principle termed as White Light Interferometer or White Light Interferometry (WLI) was developed[5]. WLI sensor systems have been used on measurands such as temperature[6,7], pressure[8] and strain[9]. For the past two years fiber optic lab. in Texas A & M University has been developing all fiber white light interferometer (AFWLI) using the configuration of Fig. 1.

White light interferometry departs from the conventional interferometry in that it uses a broadband light source. SLD in Fig.1 represents a superluminescent diode (SLD) used as a broadband light source and PD1, PD2 in Fig. 1 denote a photodetector 1 and 2 respectively.

Two fiber Fabry-Perot interferometers (FFPI) (sensing FFPI and reference FFPI in Fig. 1) and the Mach-Zehnder processing interferometer

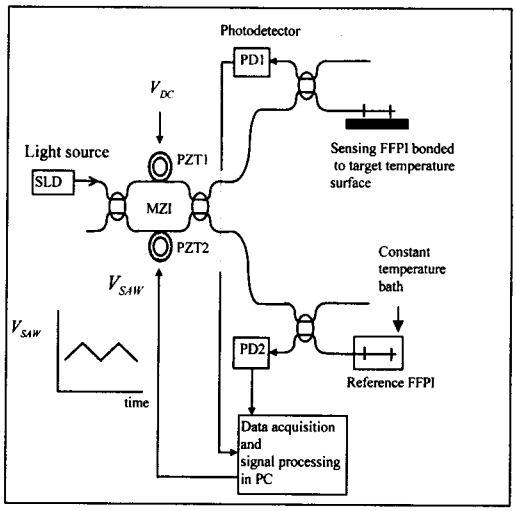

Fig.1. All Fiber White Light Interferometer

(scanning interferometer), are connected in tandem. For the case of all fiber white light interferometry, the sensing and reference interferometer output signals from photodetector 1 (Eq. 1, PD1) and 2 (Eq. 2, PD2) are given by respectively

$$I_S(\Phi_P-\Phi_S)=1+\frac{1}{2}\exp\left\{-\left[\frac{\Phi_P-\Phi_S}{\pi L_C/\lambda}\right]^2\right\}\times \cos(\Phi_P-\Phi_S) \quad (1)$$

$$I_R(\Phi_P-\Phi_R)=1+\frac{1}{2}\exp\left\{-\left[\frac{\Phi_P-\Phi_R}{\pi L_C/\lambda}\right]^2\right\}\times \cos(\Phi_P-\Phi_R) \quad (2)$$

where L_C is the coherence length of light source, Φ_p is the OPD between two arms of Mach-Zehnder processing interferometer and Φ_S , Φ_R are the round trip phase shifts for sensing interferometer, reference interferometer respectively given by

$$\Phi_P=\frac{2\pi n L_P}{\lambda} \quad (3)$$

$$\Phi_S=\frac{2\pi n L_S}{\lambda} \quad (4)$$

$$\Phi_R=\frac{2\pi n L_R}{\lambda} \quad (5)$$

Here L_P, L_S, L_R are the path length difference of the Mach-Zehnder interferometer, sensing FFPI (twice the Fabry-Perot cavity length), reference FFPI and n is the effective refractive index of core of the optical fiber. A constant d.c. voltage V_{DC} (100~150 v, Fig. 1) is applied to the PZT1 in one arm to coarsely match the OPD of MZI to that of the sensing FFPI. And an alternating ramp voltage V_{SAW} (Fig. 1) is applied to PZT2 in the other arm to scan the processing interferometer so that path length difference between two arms of MZI L_P can be varied in a certain range and also the phase of MZI Φ_P is varied in a certain range. A piezoelectric transducer (PZT2 in Fig. 1) in an arm of a scanning interferometer is used to scan the phase of processing interferometer. A zero order fringe peak is produced when the phase Φ_P and Φ_S are exactly matched. A zero order fringe peak is a peak with the highest fringe visibility (amplitude). The absolute OPD of the sensing interferometer is known if the zero order fringe peak is identified. White light interferometry has the potential to identify the interference fringe order from the output pattern of an interferometer[10]. But, for most broadband light sources, the visibility of fringes is so slowly varying in the vicinity of zero order fringe as shown in Fig. 2 and a minimum signal-to-noise ratio $SNR_{\min}$ required to identify the zero order fringe peak by simply through inspection of its magnitude is

$$SNR_{\min} = -20\log(\Delta I) = -20\log\{1-\exp[-(2/L_C)^2]\} \quad (6)$$

Representative values of coherence length of different light sources like white light lamp, Light Emitting Diode (LED), Superluminescent Diode (SLD) are about 10, 20, and 40 in terms of optical fringes. The $SNR_{\min}$ required to identify the zero order fringe by amplitude difference ΔI is given from Eq. 6 as 28 dB, 40 dB, and 52 dB respectively[11]. This requirement imposes a high minimum signal-to-noise ratio on the sensor system. This difficulty has inhibited the application of fiber optic sensors using WLI for absolute OPD determination[11].

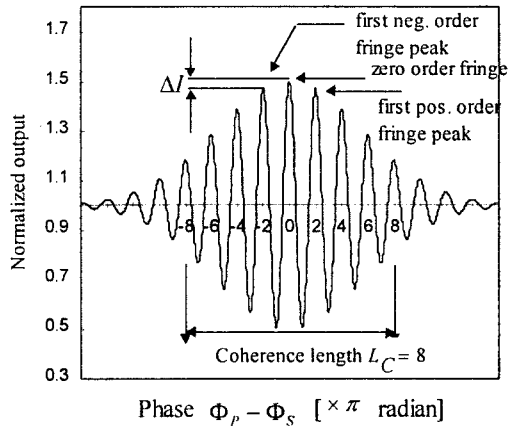

Fig. 2. Output of white light interferometer (I_S in Eq. 1)

The primary objective of this report is to develop a new signal processing algorithm which can accurately identify the zero order fringe peak from the output of a white light interferometer. The proposed signal processing algorithm uses a software approach, which is potentially inexpensive, simple and fast.

II. Previous related work

Two major classes of signal processing algorithm for WLI are the hardware approach and the software approach. Both approaches have a more or less tracking zero order fringe peak feature on which the algorithm is based. A. S. Gerges proposed hardware approach which locks the zero order fringe position of interferometer by a feedback loop[12]. The improvement of the sensitivity up to $\frac{1}{240}$ fringe was claimed. This method, while still dependent on the incremental characteristic of laser interferometry, showed the

feasibility of locking and tracking the fringe peak for absolute measurement for the first time, to the author's best knowledge.

One example of a software approach is based on tracking centroid (the center of mass)[11] of the fringe scan. This method, first, calculates centroid position (center of mass of whole fringe scan $i(m)$) m_c by using the algorithm

$$m_c = \frac{\sum |m\ i(m)|}{\sum |i(m)|} \tag{7}$$

where m is the digitized data sample number and $i(m)$ is the intensity of fringe scan. Computer simulations have shown that the centroid algorithm predicted the central fringe to ~95 % probability on a 900 test sample set with 10 % random noise. Although the centroid method allows the central fringe to be identified, it requires processing time and some features of the centroid method are only applicable to electronically scanned WLI.

III. New signal processing algorithm

This research will be focusing on the development of a new signal processing algorithm for white light interferometry. The proposed signal processing algorithm has been set to develop the signal processing algorithm for all fiber white light interferometry temperature measurement system which is shown in Fig. 1.

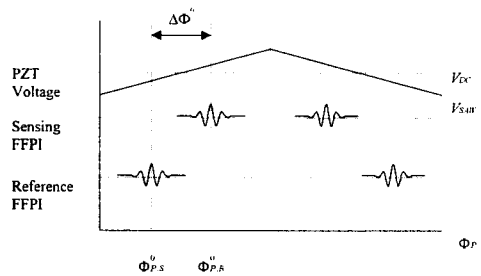

Fig. 3. Output of sensing and reference FFPI from AFWLI

This AFWLI for temperature measurement produces two fringe scans, one from sensing FFPI and another one from reference FFPI as shown in Fig. 3. First, the principle of absolute temperature measure for this AFWLI is explained as follows. In AFWLI, sensing FFPI is exposed to the temperature T_S to be measured and reference FFPI is protected from environmental disturbances but exposed to the known reference temperature T_R. Now, assume that the known temperature of the sensing FFPI and reference FFPI are T_S^0, T_R^0 respectively. When the phase of MZI Φ_P is scanned and exactly matched to that of sensing FFPI (reference FFPI), zero order fringe peak of sensing FFPI (reference FFPI) is produced at certain $\Phi_{P,S}^0$ ($\Phi_{P,R}^0$) shown in Fig. 3. In Fig. 3, $\Phi_{P,S}^0$ ($\Phi_{P,R}^0$) denotes the phase of the processing interferometer producing the zero order fringe peak of the sensing FFPI (reference FFPI). Then, the phase difference $\Delta\Phi^0 = \Phi_{P,S}^0 - \Phi_{P,R}^0$ is calculated (this is possible by the proposed signal processing algorithm which will be shown later in this report) and $\Delta\Phi^0$ is mapped (calibrated) to the temperature T_S^0. When a sensing FFPI is exposed to the another temperature T_S^i, sensor FFPI cavity length L_S is changed and the phase of processing interferometer will have its zero order fringe peak at $\Phi_{P,S}^i$. But, note that $\Phi_{P,R}^0$ is still the same because reference FFPI is protected from environmental disturbances. Now, $\Delta\Phi^i = \Phi_{P,S}^i - \Phi_{P,R}^0$ is mapped to the (absolute) temperature T_S^i. By repeating this procedures for the other temperature T_S^i, all the $\Delta\Phi^i$'s are mapped to all the sensing FFPI target temperature T_S^i. This kind of sensor is self-calibrating and is capable of absolute temperature measurement. For the purpose of temperature measurement mentioned above, reference FFPI is placed in a constant

temperature bath and sensing FFPI is bonded (or adhered) to the surface whose temperature will be measured (Fig. 1).

The main goal for the proposed signal processing algorithm is to find the phase delay between two fringe scans, $\Delta\Phi^i = \Phi^i_{P,S} - \Phi^0_{P,R}$ shown in Fig. 3 rather than to directly measure $\Phi^i_{P,S}$ and $\Phi^0_{P,R}$ individually and calculate $\Delta\Phi^i$ from $\Phi^i_{P,S}$ and $\Phi^0_{P,R}$

The proposed signal processing algorithm consists of five steps applied to sampled signal of white light interferometric fringe scans. They are;

1) Normalization and cross-correlation
2) Peak and zero crossing detection
3) Matched filtering
4) Hypothesis test
5) Fine Tuning

Each step is explained briefly below.

3.1 Normalization and cross-correlation

As a preliminary procedure, the output of photodetector signals $I_S(\Phi_P - \Phi_S)$ and $I_R(\Phi_P - \Phi_R)$ are sampled, stored in fringe scan $I_S(m)$ and $I_P(m)$ respectively and normalized to

$$i_S(m) = \frac{1}{2}\exp\left\{-\left[\frac{2\pi(m - m_s)/f_S}{\pi L_C/\lambda}\right]^2\right\}\times \cos\{2\pi(m - m_s)/f_S\} + X(m) \quad (8)$$

and

$$i_R(m) = \frac{1}{2}\exp\left\{-\left[\frac{2\pi(m - m_R)/f_S}{\pi L_C/\lambda}\right]^2\right\}\times \cos\{2\pi(m - m_R)/f_S\} + Y(m) \quad (9)$$

respectively where m_s is zero order fringe peak sample number for sensing FFPI, m_R is zero order fringe peak sample number for reference FFPI, f_S is the sample rate [samples per fringe] and $X(m)$, $Y(m)$ are the white noise related to the fringe scan $i_S(m)$, $i_R(m)$ respectively. The phase difference $\Delta\Phi^i$ between sensing FFPI and reference FFPI is defined in terms of samples as

$$m_d = m_S - m_R \quad (10)$$

A normalization procedure is carried out by removing the d.c. component (constant 1 in Eq. 1,2) of each fringe scan. A normalization procedure is used to find the zero crossing period of a fringe. After normalization, $i_s(m)$ and $i_R(m)$ are cross-correlated into $i(m)$ and (normalized) cross-correlation function $i(m)$ can be expressed in mathematical form as

$$i(m) = \sum_{k=\infty}^{\infty} i_R(k)\, i_S(m+k) = \frac{1}{2}\exp\left\{-\left[\frac{2\pi(m - m_d)/fs}{\pi L_{C,eff}/\lambda}\right]^2\right\}\times \cos\{2\pi(m - m_d)/f_s\} + W(m) \quad (11)$$

In Eq. 11, the effective coherence length $L_{C,eff}$ is given as $\sqrt{2}L_C$[13] and $W(m)$ is a white noise of $i(m)$. Exponential term in Eq. 11 is termed as "the envelope" of cross-correlation function $i(m)$. Note that the cross-correlation function $i(m)$ has a peak value (best similarity) at $m = m_d$ This m_d corresponds to the phase difference $m_d = m_S - m_R$ between sensing FFPI and reference FFPI and $i(m)$ has a same period of modulated cosine function as the one of both $i_R(m)$ and $i_S(m)$. This cross-correlation improves SNR at zero order fringe peak up to 14 dB[13]. The cross-correlation therefore exhibits the increased SNR at the zero order fringe peak. One disadvantage related to cross-correlation is the broadening of peak due to the cross-correlation of two (almost) identical Gaussian functions so that coherence length is increased up to $\sqrt{2}L_C$[13, 14]. This results in higher SNR_{min} in Eq. 6 requiring 6 dB more than before cross-correlation when $L_C = 26\lambda$ but this will be compensated by the result of less noisy $i(m)$ than either of $i_S(m)$ or $i_R(m)$ and 14 dB SNR improvement at the zero

order fringe peak [13]. After cross-correlation, the task of the signal processing algorithm becomes to find a zero order fringe peak (global maximum) of cross-correlation function $i(m)$ correctly.

3.2 Peak and zero crossings detection

At this stage, all the peaks and minima positions of the cross-correlation function $i(m)$ are detected and registered. Every peak positions is labeled as $m=p_i$ where $p_0=m_d$ is zero order fringe peak, p_{-1} is negative first order fringe peak, p_1 is positive first order fringe peak and so on. Also every zero position between peak and minimum is detected and registered as z_i where $i=\ldots,-2,-1,1,2,\ldots$ Then the zero crossing period b is calculated by applying Least Squares Fitting to the distance between all pairs of zero (z_i and z_{i+1}) and $2\hat{b}$ is denoted by $\hat{f}_S$, the estimated sample rate.

3.3 Matched filtering and SNR improvement at peaks

A matched filter is the optimum filter to maximize the SNR[14]. For our application, the matched filter is one fringe of a cosine function and one fringe of cross-correlation $i(m)$ is the signal to be matched. SNR of cross-correlation between the matched filter and signal to be matched is maximized when the time delay between two signal is zero. SNR-improved peaks are

$$J_i=\sum_{p_i}^{p_{i+1}} i(m)\cos\left(\frac{2\pi m}{2b}\right)$$
$$\cong\sum_{p_i}^{p_{i+1}}\left\{h_i\cos\left(\frac{2\pi m}{f_s}\right)+W(m)\right\}\cos\left(\frac{2\pi m}{2b}\right) \quad (12)$$

where h_i is the average value of exponential envelope function between p_i and p_{i+1} in Eq. 12. In this stage, $i(p_i)$ is replaced by J_i and SNR at the zero order fringe peak can be improved by 5[dB] using matched filtering[11]. One useful property of J_i is $J_0=J_{-1}$, $J_1=J_{-2}$ ...$(J_i=J_{-i-1})$ due to the symmetric property of $i(m)$.

3.4. Hypothesis test

Signal processing algorithm chooses the nine biggest peaks (p_j, $j=0,\pm1,\pm2,\pm3,\pm4$) as zero order fringe peak candidates. Hypothesis test presumes each candidate peak is the zero order fringe peak and calculate the parameter $g(p_j)$

$$g(p_j)=\sum_{i=0}^{\infty}(J_{j+i}-J_{j-i-1})$$
$$=\sum_{i=0}^{\infty}d(j,i) \quad (13)$$

where j corresponds to the candidate peak p_j, on the hypothesis test and i is the distance from the zero order fringe peak candidate in terms of fringe. Then, for example, $g(p_0)$ is expressed as

$$g(p_0)=d(0,0)+d(0,1)+d(0,2)+\ldots\ldots$$
$$=(J_0-J_{-1})+(J_1-J_{-2})+(J_2-J_{-3})+\ldots \quad (14)$$

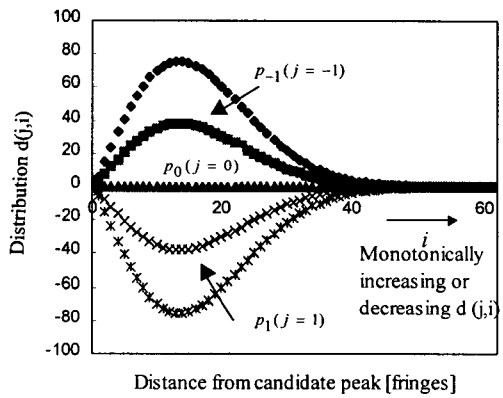

Fig. 4. Distribution $d(j,i)$ of noise-free fringe scan

Ideally all the values of $d(j=0,i)$for the zero order fringe peak p_0 is zero (Fig. 4) due to the property of $J_i=J_{-i-1}$ and the zero order fringe peak candidate producing minimum $|g(p_j)|$ is announced as the zero order fringe peak.

3.5 Fine tuning

The discrete sample zero order fringe peak position of $i(m)$, $p_d = m_d$ identified by hypothesis test is not necessarily same as true zero order fringe peak position , $p_i = p_0$ (Fig. 5).

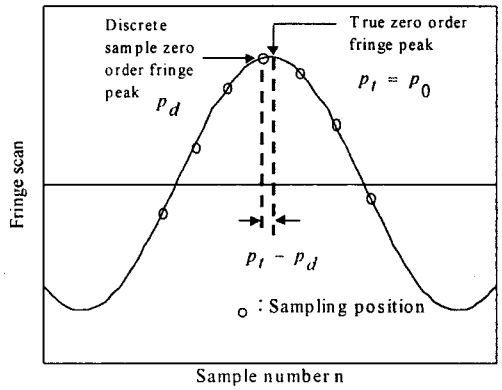

Fig. 5. Vicinity of zero order fringe peak (cross-correlation function $i(m)$)

Assuming that cross-correlation function $i(m)$ is represented as

$$i(m) = \frac{1}{2}\exp\left\{-\left[\frac{2\pi(m-p_t)/f_S}{\pi L_{C,eff}/\lambda}\right]^2\right\}\times \cos\left\{\frac{2\pi(m-p_t)}{f_S}\right\} \quad (15)$$

and the approximate value of coherence length of light source, $\hat{L}_C$ is known to us beforehand, fine tuning algorithm generates test fringe scan

$$i_{test}(m) = \frac{1}{2}\exp\left\{-\left[\frac{2\pi(m-p_d)/\hat{f}_S}{\pi \hat{L}_{C,eff}/\lambda}\right]^2\right\}\times \cos\left\{\frac{2\pi(m-p_d)}{\hat{f}_S}\right\} \quad (16)$$

$\hat{L}_{C,eff}$ in Eq.15 is given as $\sqrt{2}\hat{L}_C$ Time shift between p_d and p_i can be found by calculating the cross-correlation $J(M)$

$$J(M) = \sum_{m=-\infty}^{\infty} i(m)\, i_{test}(m - M\triangle m) \quad (17)$$

for varying integer number M and

$$\triangle m = \frac{1}{N_{sub}} \quad (18)$$

N_{sub} is the number of sub-divisions in one fringe and Δm is the desired sub-fringe resolution. Then $J(M)$ becomes

$$J(M) = \sum_{m=-\infty}^{\infty}\frac{1}{2}\exp\left\{-\left[\frac{2\pi(m-p_t)/f_S}{\pi L_{C,eff}/\lambda}\right]^2\right\}\times \cos\left\{\frac{2\pi(m-p_t)}{f_S}\right\}\times \frac{1}{2}\exp\left\{-\left[\frac{2\pi(m-p_d-M\triangle m)/\hat{f}_S}{\pi \hat{L}_{C,eff}/\lambda}\right]^2\right\}\times \cos\left\{\frac{2\pi(m-p_d-M\triangle m)}{\hat{f}_S}\right\} \quad (19)$$

Note that the zero order fringe peak $m = p_d + M\Delta m$of test fringe scan $i_{test}(m - M\Delta m)$ varies for changing M and cross-correlation $J(M)$ has a peak value at the certain M_F which makes $M_F\Delta m \approx (p_t - p_d)$ Then fine tuning algorithm announces $(p_d + M_F\Delta m)$ which maximizes $J(M)$, as the estimated true zero order fringe peak location $\hat{p}_t$ The true zero order fringe peak p_t is usually within half sample of the discrete zero order fringe peak p_d and $J(M)$ is calculated over the range from $M = -\frac{N_{sub}/f_S}{2}$ to $M = -\frac{N_{sub}/f_S}{2}$ for faster signal processing.

IV. Computer Simulations

The proposed signal processing algorithm was verified using computer simulations. To see the shot-noise limited performance of proposed signal processing algorithm, the normalized WLI fringe scans, $i_S(m)$ and $i_R(m)$ were computer-generated using Eq. 8 and Eq. 9 respectively and shot noise was added to the WLI fringe scans, $i_S(m)$ and $i_R(m)$ instead of white noise. In the computer simulation the zero order fringe peak position p_0 for $i_S(m)$ was randomly selected

between $-5<p_0<5$. Same procedures were repeated for $i_R(m)$. $i_S(m)$ and $i_R(m)$ were cross- correlated into $i(m)$ and the coherence length of $i_S(m)$ and $i_R(m)$ were chosen as $L_C=26\lambda$ to simulate the coherence length of the SLD used in the AFWLI shown in Fig. 1. For all the simulations presented in this report parameters are fixed as follows unless the specified parameter is varied for a certain range.

. Sample rate $f_s=16$ samples/fringe

. SNR =30 dB

. Coherence length $L_{C,eff}=36\lambda$

. Size of sub-fringe resolution Δm=1/1000 fringe

4. 1. Simulation: Miss rate simulation

In the first simulation miss-rate (misident-ification rate) of the proposed algorithm was tested at different shot noise levels. The SNR was varied from 1 dB to 28 dB with 1 dB separation and a set of 10000 simulations was carried out at a given SNR. When the position difference between the calculated zero order fringe peak and the computer-generated zero order fringe peak is bigger than half fringe (8 samples), the zero order fringe peak is considered to have been misidentified. Table 1 shows the miss rate of the proposed signal processing algorithm and miss rate is the rate of number of miss to 10000.

In Fig. 6, miss rate was plotted along with Bit Error Rate (BER) of binary fiber optic communication system[15]. Note that the miss rate curve in Fig. 6 covers only up to the miss rate at 28 dB SNR and miss rate at 29 ~ 32 dB SNR in Table 1 are not seen in Fig. 6. In Fig. 6 (or Table 1) we have a rule of thumb that every dB improvement in SNR (over the range of 26 ~ 31 dB) produces approximately one orders of magnitude improvement in error rate. This kind of behaviour is also the case for binary fiber optic communication system (two orders of magnitude improvement in error rate for the

Table 1. Miss rate of the proposed signal processing algorithm as a function of SNR

SNR [dB]	Miss Rate	SNR [dB]	Miss Rate
1	0.95	17	0.46
2	0.94	18	0.40
3	0.93	19	0.34
4	0.91	20	0.30
5	0.89	21	0.23
6	0.87	22	0.19
7	0.85	23	0.14
8	0.83	24	0.10
9	0.80	25	0.066
10	0.76	26	0.041
11	0.73	27	0.019
12	0.69	28	0.009
13	0.64	29	0.004
14	0.60	30	0.001
15	0.56	31	0.0003
16	0.51	32	0

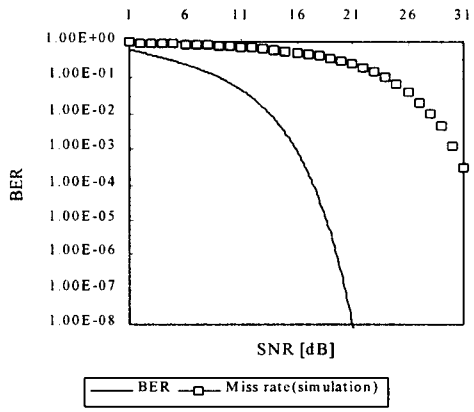

Fig. 6. Comparison between miss rate and BER.

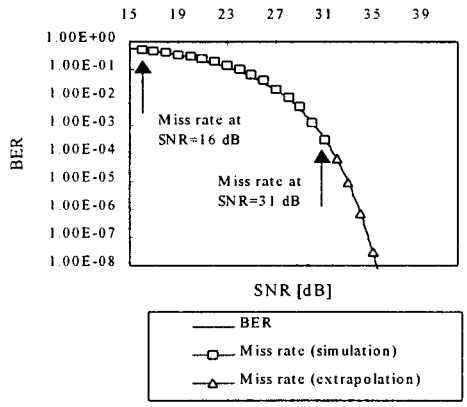

Fig. 7. Extrapolation of miss rate on BER curve.

binary fiber optic communication system). To extrapolate the miss rate beyond the range of 10^{-4} on the BER curve, data points in abscissa in Fig. 6 were left-shifted by ~14.2 dB (by trial and error) until data points of miss rate between 16 dB ~ 31 dB were visually fitted on the BER curve. Then four more data points were extrapolated after the data point of miss rate at 31 dB SNR on the BER curve as shown in Fig. 7. It is predicted that miss rate will be 3×10^{-8} at SNR of 35 dB.

4.2. Root mean square (RMS) error of the zero order fringe peak identification

After the zero order fringe peak was identified fine tuning was carried out for resolution enhancement. Phase error $\Phi_{error,i}$ between computer generated zero order fringe peak and fine-tuned zero order fringe peak was calculated. Phase error $\Phi_{error,i}$ was averaged over 30 simulations at a given SNR and this average gives out the root mean square (RMS) error Φ_{RMS} of the zero order fringe peak identification.

$$\Phi_{RMS}=\sqrt{\frac{\sum_{i=1}^{30}(\Phi_{error,i})^2}{30}} \quad (20)$$

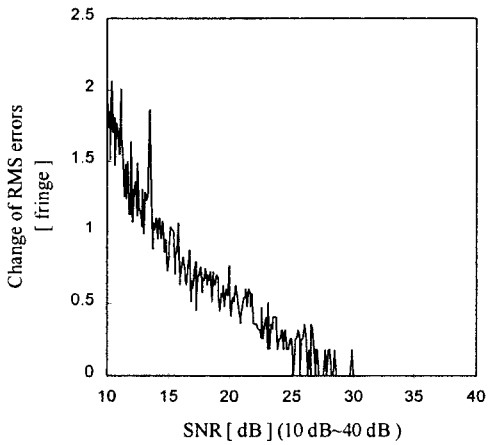

Fig. 8. Change of RMS error as a function of SNR (10~40 dB).

Fig. 8 shows the change of RMS error along the SNR in the range of 10 dB to 40 dB and Fig. 9 shows the change of RMS error along the SNR in the range of 30 dB to 40 dB. It is shown that the minimum SNR required to achieve RMS error less than 10^{-3} fringe is 35 dB. For the temperature measurement application RMS error less than 10^{-3} [fringe] corresponds to the 0.006 deg. C for 10 mm FFPI cavity length [13].

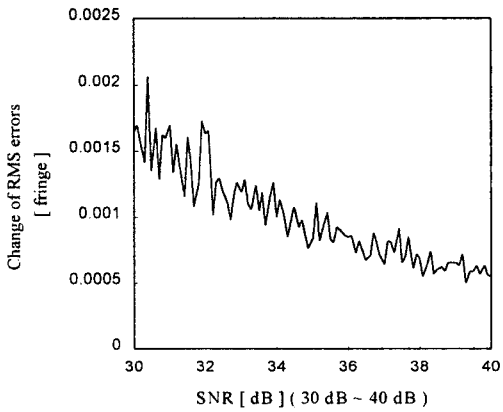

Fig. 9. Change of RMS error as a function of SNR (30~40 dB).

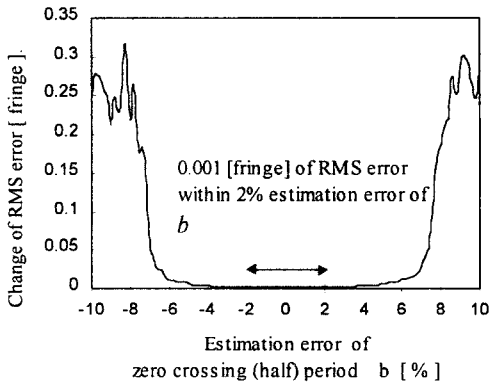

Fig.10. Change of RMS error as a function of estimation error in zero crossing period.

4.3. Simulation: Effects of $\hat{b}(\hat{f}_S)$

In this simulation, estimated coherence length $\hat{L}_{C,eff}$ was set as 36 fringes and estimation error

of $\hat{b}$ was varied from -10% to 10% when $b=10$ ($2b=\hat{f}_S=20$samples/fringe) and SNR=30 dB. For the estimation error $\hat{b}$ in the range from -6 % to 6 % in Fig. 10, RMS error was not sensitive to the $\hat{b}$, but around the ±7 % error of $\hat{b}$ the cross-correlation $i(m)$ and test fringe scan (Eq. 16) started being out of phase and RMS error increased fast.

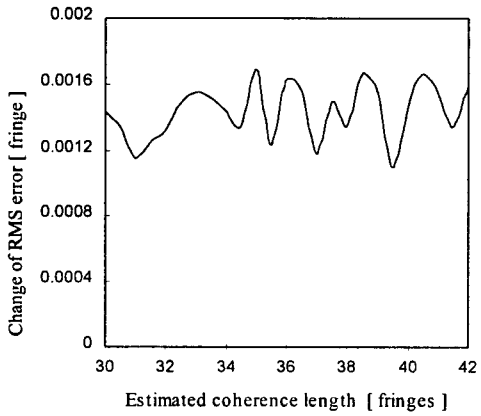

Fig. 11. Change of RMS error as a function of estimation error in coherence length.

4.4. Simulation: Effects of $\hat{L}_C$

This simulation is to show the effect of estimated coherence length $\hat{L}_C$ on RMS error when $\hat{b}=b$. SNR was fixed as 30 dB. Estimated coherence length $\hat{L}_{C,eff}$ was varied from 30λ to 42λ and RMS error was observed. Fig. 11 shows that RMS error is not sensitive to the estimation error in coherence length $\hat{L}_{C,eff}$. This is due to the property of cross-correlation. Cross-correlation is maximized when p_t and $p_d+M\Delta m$ are in phase as long as the cross-correlation $i(m)$ and test fringe scan signal is symmetric.

V. Conclusions

A new signal processing algorithm for white light interferometry has been proposed. This signal processing algorithm was initially developed for the all fiber white light interferometer (AFWLI) developed at Texas A & M University. AFWLI produces two fringe scans. The goal of signal processing algorithm was to find the time delay (phase shift) between two fringe scans which makes it possible to measure the absolute optical path length of a sensing interferometer. This new signal processing algorithm can be used for absolute temperature measurement by mapping the zero order fringe peak position of cross correlation function to the time delay between two fringe scan. Cross-correlation between two fringe scans utilizes all the photons in fringe scans effectively and the uncertainty of the zero order fringe peak misidentification was reduced. Computer simulations showed that the proposed signal processing algorithm identified the zero order fringe peak with a miss rate of 0.0003 at 31 dB shot noise and the extrapolated miss rate at 35 dB shot noise was 3×10^{-8}. Also, at 35 dB shot noise, resolution of 10^{-3} fringe was obtained (Fig. 9). The signal processing algorithm requires a prior knowledge about the coherence length of the SLD, L_C and sample rate f_S. But the performance of proposed signal processing algorithm turned out to be not sensitive to the estimation error in $\hat{L}_C$ and $\hat{f}_S$ (within the range from -6% to 6% estimation error of $\hat{b}$). The proposed signal processing algorithm uses a software approach which is potentially inexpensive, simple and fast. As a whole, the proposed signal processing algorithm has proven to be effective for AFWLI temperature measurement.

Acknowledgement

This research was supported by the Hansei University.

References

[1] T.G. Giallorenzi, J.A. Bucaro, A.Dandridge, G.H. Sigel, Jr., J.H. Cole, S.C. Rashleigh, and R.G. Priest, "Optical fiber sensor technology", *IEEE Journal of Quantum Electronics*, vol. QE-18, pp.626-665, Apr. 1982.

[2] E. Udd (ed), *Fiber optic sensors*, New York: Wiley, 1991.

[3] A.D. Kersey, A.Dandridge, "Applications of fiber-optic sensors", *IEEE transactions on Components, Hybrids and Manufacturing technology*, v.13, n.1, Mar., 1990, pp.137-143.

[4] Kim D. Jovanovich, "Fiber optic sensing applications in the electric power industry", *Electric Power System Research*, 30 (1994) pp. 215-221.

[5] H.C. LeFerve, "White-light interferometry in optical fibre sensors", *Proceedings of 7th Optical Fibre Sensors Conference*, pp. 345-352.

[6] C. Lee and H.F. Taylor, "Fiber-optic Fabry Perot temperature sensor Using a low-coherence light source", *Journal of Lightwave Technology*, v.9, n.1, Jan., 1991, pp.129-134.

[7] S. C. Kaddu, S. F. Collins, D. J. Booth, "A large operating range fibre temperature sensor employing low coherence interferometry," *Australian Conference on Optical Fibre Technology* 94, pp.150-153.

[8] W. J. Bock et al, "White-light interferometric fiber-optic pressure sensor", *IEEE Transactions on Instrumentation and Measurement*, v.44, n.3, June 1995, pp.694 -607.

[9] G. Zuliani et al, "Demodulation of a fiber Fabry-Perot strain sensor using white light interferometry, SPIE vol. 1588, *Fiber Optic Smart Structures and Skins* IV, p. 308-313, 1991.

[10] K.T.V Grattan, B.T. Meggitt (ed), *Optical fibre sensor technology*, London: Chapman & Hall, 1995.

[11] S.Chen et al, "Digital signal processing techniques for electronically scanned optical -fibre white light interferometry", *Applied Optics*, Vol.31, No.28, October, 1992, pp.6003 -6010.

[12] A.S. Gerges et al, "Interferometric fibre-optic sensor using a short-coherence-length source", *Electronics Letter 8th* October 1987 Vol.23 No.21.

[13] Jeong Gon Kim, "A new signal processing algorithm for white light interferometry", Ph.D. Dissertation, Texas A & M University, College Station, Texas, 1997.

[14] G.R. Cooper, C.D. McGillem, *Probabilistic methods of signal and system analysis*, New York: Holt, Rinehart and Winston, 1986.

[15] P. Green, Jr., *Fiber optic networks*, Englewood Cliffs, New Jersey:Prentice-Hall, 1993.

著 者 紹 介

Jeong Gon Kim received the B.S.E.E. degree from Yonsei university, Seoul, Korea and M.S.E.E. degree and Ph.D. degrees from Georgia Institute of Technology, Atlanta, U.S.A. and Texas A &M University, Texas, U.S.A. in 1982, 1989, 1997 respectively. He joined the department of Information and Communication Engineering, Hansei University in 1998 where he is currently an assistant professor. His current research interests are in fiber optic sensor, fiber optic communication and computer network.